 

*CONFERENCES AND SYMPOSIA*

PACS numbers: 75.10.Jm, 75.10.Pq, 75.40.Gb

90th ANNIVERSARY OF THE P.L. KAPITZA INSTITUTE FOR PHYSICAL PROBLEMS, RUSSIAN ACADEMY OF SCIENCES

# Fermi liquid of spinons in quasi-one-dimensional antiferromagnets *

A.I. Smirnov

DOI: https://doi.org/10.3367/UFNe.2024.12.039842

## Contents



**Abstract. We report the experimental observation of a shift of the boundaries of the spinon continuum caused by a Fermi-liquid interaction of spinons in the spin-liquid $S = 1/2$ chain-type antiferromagnet $K_2CuSO_4Br_2$. The parameter of spinon interaction, which determines the probability of backscattering, is found. In the pseudospin $S = 1/2$ chain-type strongly anisotropic antiferromagnet $Cs_2CoCl_4$, a shift in the magnetic resonance frequency is detected during the crossover from the disordered spin regime to the state of correlated XXZ-type spin chains at a temperature above the emergence of long-range antiferromagnetic order. This resonance shift is explained on the basis of the spectrum of spin excitations in correlated XXZ chains and corresponds to theoretical simulation of the spectra of spinon-type magnetic fluctuations in XXZ chains [P. Laurell et al. *Phys. Rev. Lett.* 127 037201 (2021)].**

**Keywords:** spin chains, spinons, spin liquids, magnetic resonance, antiferromagnets, quantum magnets

## 1. Introduction. Ground state and excitations of one-dimensional $S=1/2$ antiferromagnetic chain

One-dimensional spin chains may be realized in many dielectric magnetic crystals enabling one to investigate the states of these multiparticle objects demonstrating purely quantum properties, with their states being unexpected from classical points of view. In this area, much theoretical work has been done and experimental studies have been carried out on many substances. In this review, we will present new experimental results on the study of ground states and excitation spectra in one of the most simply formulated models, $S = 1/2$ antiferromagnetic spin chains. A new result is the observation of excitation spectra that are characteristic of the Fermi liquid of quantum multiparticle excitations.

Let us first describe the basic concepts of quantum $S = 1/2$ spin chains with an antiferromagnetic Heisenberg exchange of nearest neighbors. The initial Hamiltonian of this system has the form

$$\mathcal{H} = \sum_i J\mathbf{S}^i\mathbf{S}^{i+1}, \tag{1}$$

where $J > 0$ is the exchange integral, and $\mathbf{S}^i$ is the $S = 1/2$ spin operator at a lattice site.

In a theoretical study of this model (see, for example, [1–3]), it was shown that the ground state of the chain is disordered in the classical sense, i.e., the average values of spin projections at all chain sites are zero: $\langle S_\alpha^i \rangle = 0$, $\alpha = x, y, z$. Nevertheless, this state turns out to be strongly correlated with an infinite correlation radius, and the antiferromagnetic correlations of the spins decrease in a power-law manner:

$$\langle S_z^i S_z^{i+k} \rangle \sim \frac{(-1)^k}{k}. \tag{2}$$

This behavior of correlations allows this ground state to be called quantum-critical. The temperature dependence of the susceptibility has a maximum at a temperature of the order of $J/k_B$ [4] but exhibits no critical features. Faddeev and Takhtajan [2, 5] obtained an important result on the way to understanding the structure of the ground state and elementary excitations in one-dimensional antiferromagnetic chains. They showed that delocalized dynamic domain-wall-type structures in an antiferromagnet are close to a solution to the problem of eigenstates. An alternating series of ordered

**A.I. Smirnov.** Kapitza Institute for Physical Problems, Russian Academy of Sciences, ul. Kosygina 2, 119334 Moscow, Russian Federation
E-mail: smirnov@kapitza.ras.ru

Received 18 December 2024
*Uspekhi Fizicheskikh Nauk* **195** (7) 778 – 786 (2025)
Translated by I.A. Ulitkin

* Joint meeting of the Scientific Session of the Physical Sciences Division of the Russian Academy of Sciences and the Scientific Council of the Kapitza Institute for Physical Problems of the Russian Academy of Sciences, dedicated to the 90th anniversary of the Kapitza Institute for Physical Problems, Russian Academy of Sciences (December 18, 2024) (see *Phys. Usp.* **68** (7) 699 (2025); *Usp. Fiz. Nauk* **195** 747 (2025)).

spins (up, down, up, down, etc.) fails on such walls. Such excitations distinguish spin chains from ordinary three-dimensional antiferromagnetic structures, where elementary excitations are magnons, for the description of which one flipped spin is considered one the background of an antiferromagnetically ordered structure. In a spin chain, one flipped spin generates an increase in the exchange energy on two exchange bonds to the right and left of it. An excitation in the form of one flipped spin in a spin chain splits into two domain boundaries when each of the two spins in a pair adjacent on the right or on the left to the already flipped spin is rotated by 180°. In this case, the exchange energy and the total spin of the chain do not change. The domain boundaries can move without energy loss due to the described rotations. Comparative schematic diagrams of such excited states are given, for example, in [6] and in the Supplemental material to paper [7]. Thus, two domain boundaries have the same energy in the Ising approximation as an ordinary magnon and the same total spin $S = 1$. On this basis, it was natural to assign the $S = 1/2$ spin to the elementary excitations of the chain and to consider them to be fermions. They were called spinons. This gave rise to the idea of the impossibility of individual excitation of spinons in neutron scattering or photon absorption processes, since, in these processes, the change in the projection of the neutron or photon spin must be equal to unity.

Energy transfer to spinons in two-particle or many-particle processes results in a continuum neutron scattering spectrum, where, for each value of the transferred momentum, there is an extended interval of transferred energy values. Let us consider the processes of energy transfer to a spinon–fermion system at a qualitative level. We will use the expression for the energy of a spinon with a wave vector $q$, obtained by transforming the original spin Hamiltonian to fermion $S = 1/2$ operators (see, for example, [3, 7, 8] and the Supplemental material to paper [7]). In this case, a simplifying assumption is made based on the mean field approximation to take into account the correlations of spins at neighboring sites, with the terms corresponding to the interaction of fermions being ignored. The number of fermions is equal to the number of spins in the chain. Thus, spinons in the ground state fill half the Brillouin zone. The ground state consists of delocalized spinons propagating along the chain. In the approximation of free fermions, their dispersion law has the form

$$\varepsilon_0(q) = -\gamma J \cos(qa), \tag{3}$$

where $a$ is the chain period, and $\gamma$ is a dimensionless parameter which, in accordance with the analytical calculation of the lower boundary of the continuum [9], should be taken to be $\gamma = \pi/2$. In the presence of an external magnetic field, the states of spinons with opposite spin projections are split, and fermions with positive and negative projections of the magnetic moment have the energies

$$\varepsilon_\pm(q) = -\gamma J \cos(qa) \pm \mu_B H. \tag{4}$$

Figure 1 shows these dispersion laws. To construct a continuum of neutron scattering or photon absorption in the free spinon approximation (Fermi gas approximation), we should keep in mind the ground state with all states filled below the Fermi level $\varepsilon_F = 0$, with excitations being treated as

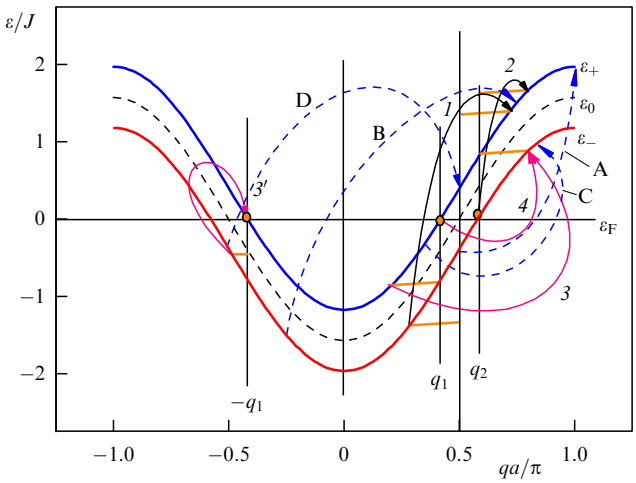


**Figure 1.** Dispersion law of free spinons in magnetic field $H = \pi J/(8\mu_B)$. Solid arrows indicate transitions that form boundaries of excitation continuum, and dashed arrows correspond to transitions within continuum (see text). Orange segments represent parameter $\delta$, with a change in which transition moves along boundary of continuum shown in Fig. 2.

states of the 'quasiparticle plus hole' type when a spinon from the filled part of the Fermi sphere undergoes a transition into a free state with an energy above the Fermi level. Of all such transitions, we will be interested in the transitions between the branches $\varepsilon_-$ and $\varepsilon_+$ or between $\varepsilon_+$ and $\varepsilon_-$ for electron spin resonance (ESR) experiments, because the spin projection of the chain changes by $\pm 1$ in them, as required by the selection rules for the absorption of a quantum of the electromagnetic field. These are transitions whose matrix elements are provided by oscillations of the spin components transverse to the field. The upper energy limit of such excitations on the $(ka, \varepsilon)$ plane is obtained in transitions of type *1* (see Fig. 1) between the states $\varepsilon_-(\pi/2 - \delta) \to \varepsilon_+(\pi/2 + \delta)$ and is shown by curve *1* in Fig. 2. Hereinafter, $\delta$ is a positive parameter shown in Fig. 1 as orange horizontal segments. When $\delta$ changes from zero, the position of the ends of the line with the arrow changes, determining a change in the energy limit value as a function of the excitation wave vector $k$. The lower energy limit for transitions from the $\varepsilon_-$ branch to the $\varepsilon_+$ branch is set by the transitions indicated by arrow *2* in Fig. 1: $\varepsilon_-(q_2) \to \varepsilon_+(q_2 + \delta)$. In Figure 2, this limit is demonstrated by curve *2*. Hereinafter, $q_{1,2}$ are the wave vectors of spinons at the Fermi level with the upward and downward projection of the magnetic moment, respectively; they are shown in Fig. 1 by vertical lines. The upper energy limit for $\varepsilon_+ \to \varepsilon_-$ transitions is determined by $\varepsilon_+(q_1 - \delta) \to \varepsilon_-(q_2 + \delta)$ transitions (arrow *3* in Fig. 1 and curve *3* in Fig. 2). The lower energy limit for $\varepsilon_+ \to \varepsilon_-$ transitions is determined by transitions $\varepsilon_+(q_1) \to \varepsilon_-(q_2 + \delta)$ (arrow *4*). The falling branch of zero-width excitations is associated with the $\varepsilon_-(-q_1 - \delta) \to \varepsilon_+(-q_1)$ transitions (arrow *3′*), $\delta \leqslant q_2 - q_1$. The frequencies of the transitions falling inside the continuum are designated by the letters A, B, C, and D in Fig. 2; in Fig. 1, these transitions are designated by dashed arrows with the corresponding letters.

Thus, the spectrum of transferred neutron energies or absorbed photon energies has the form of the continuum shown in Fig. 2; it is called a spinon or a two-spinon continuum. For ESR spectroscopy (at $k = 0$) based on this spectrum, we expect absorption only at the Larmor frequency

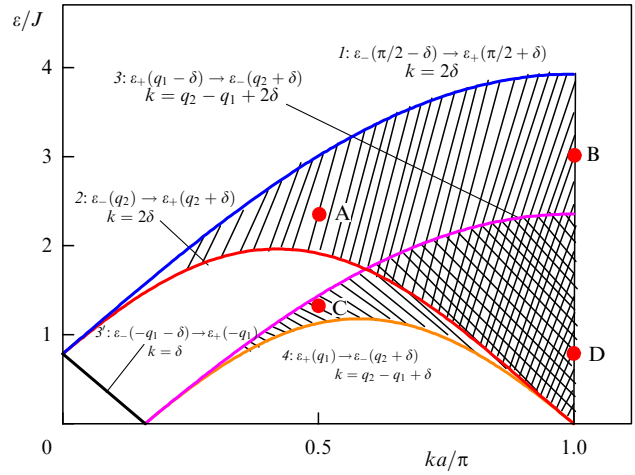


**Figure 2.** Continuum of transverse spin fluctuations in magnetic field. Right half of Brillouin zone is shown.

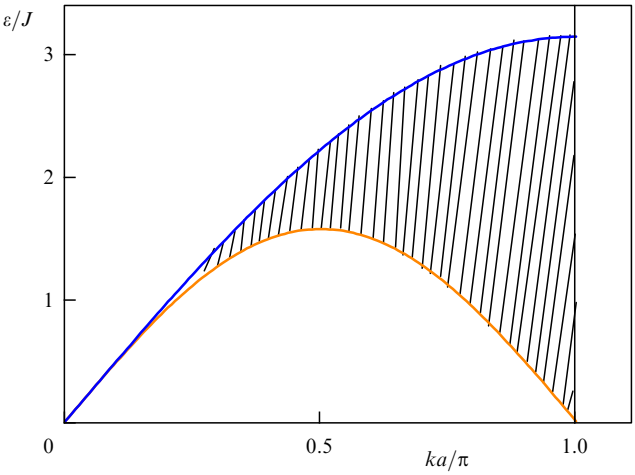


**Figure 3.** Two-spin continuum in zero field.

$\omega_{\rm L} = g\mu_{\rm B}H/\hbar$, as in the case of ordinary paramagnetic resonance. In the absence of an external field, the splitting of the spinon spectra disappears and the form of the continuum is simplified, which is shown in Fig. 3. This form of the continuum has been repeatedly observed in experiments on inelastic neutron scattering with quasi-one-dimensional antiferromagnets (see, for example, [10–12]). Also, in experiments on inelastic neutron scattering, a modification of the continuum in a magnetic field was observed. In a magnetic field, soft modes of spin oscillations with $\Delta S_z = 0$ were detected on wave vectors $k = 2q_{1,2}$ on both sides of $\pi/a$ [3], i.e., excitations of the form $\varepsilon_+(-q_1) \to \varepsilon_+(q_1)$ and $\varepsilon_-(-q_2) \to \varepsilon_-(q_2)$.

In contrast to the purely Heisenberg case, in antiferromagnetic chains with a uniform Dzyaloshinskii–Moriya interaction (DMI) [13, 14], the spinon nature of the continuum manifests itself in the ESR [15]. The Hamiltonian of the chain in a magnetic field and in the presence of the specified interaction takes the form

$$\mathcal{H} = \sum_i \left( J\mathbf{S}^i\mathbf{S}^{i+1} + \mathbf{D}\,\mathbf{S}^i \times \mathbf{S}^{i+1} + g\mu_{\rm B}\mathbf{S}^i\mathbf{H} \right). \qquad (5)$$

Here, the vector $\mathbf{D}$ is the DMI parameter.

The authors of [15–17] showed that, in the presence of a homogeneous DMI, spinons propagating in opposite directions acquire opposite shifts of their eigenfrequency, and the degeneracy of the energies of these two spinons is removed. As a result, instead of one value of the ESR frequency in the form of the Larmor frequency, a so-called spinon doublet arises, the splitting of which in frequency corresponds to the distance between the upper and lower boundaries of the continuum of the Heisenberg chain on the wave vector $q_{\rm DM} = D/Ja$. This result also follows from the fact that, at $\mathbf{H} \parallel \mathbf{D}$, the spinon spectrum in the presence of a homogeneous DMI shifts along the wave vector by $\pm q_{\rm DM}$ [17], and the ESR frequencies acquire values for the field orientations $\mathbf{H} \parallel \mathbf{D}$ and $\mathbf{H} \perp \mathbf{D}$ having the form

$$2\pi\hbar\nu_\pm = \left| g_\parallel \mu_{\rm B} H \pm \frac{\pi D}{2} \right|, \qquad (6)$$

$$2\pi\hbar\nu_\pm = \sqrt{(g_\perp \mu_{\rm B} H)^2 + \left(\frac{\pi D}{2}\right)^2}. \qquad (7)$$

Here, $g_{\parallel,\perp}$ are the values of the $g$-factor for $\mathbf{H} \parallel \mathbf{D}$ and $\mathbf{H} \perp \mathbf{D}$. Relations (6) and (7) determine the ESR gap in a zero field, $2\pi\hbar\nu_\pm^0 = \pi D/2$, and predict the presence of a soft mode for $\mathbf{H} \parallel \mathbf{D}$ in a magnetic field $H_0 = \pi D/(2g_\parallel \mu_{\rm B})$. This soft mode is equivalent to the zeroing of the excitation frequency in the continuum of the Heisenberg chain on the wave vector $k = q_2 - q_1$ (see Fig. 2).

A doublet of ESR lines, $\nu_\pm$ at $\mathbf{H} \parallel \mathbf{D}$, was indeed observed, for example, in $K_2CuSO_4Br_2$ crystals and other quasi-one-dimensional magnets [6, 18]. Figure 4a shows ESR lines at three different frequencies. Figure 4b illustrates the above-described scheme of the formation of a doublet of resonance frequencies during DMI, which shifts the spectrum in the $k$-space or, in other words, transfers the ESR from the zero wave vector to the wave vector $q_{\rm DM}$. The $K_2CuSO_4Br_2$ crystal [19] is very suitable for studying the spinon doublet by the ESR method, because it almost ideally behaves according to the model of one-dimensional spin chains (the intrachain-to-interchain exchange ratio is 600), the magnetic $Cu^{2+}$ ions carry a spin of $S = 1/2$, and the symmetry allows the presence of a uniform DMI in the chains. The ESR experiments in $K_2CuSO_4Br_2$ [18] show very good agreement with the results of the spinon doublet theory in the Fermi gas of spinons. With decreasing temperature, a doublet is formed, and a soft ESR mode is detected in the field $H = \pi D/2g\mu_{\rm B}$. The frequency-field dependence of the components of the ESR spinon doublet in low fields corresponds to the theoretical dependence (6). This correspondence is shown in Fig. 5; the plot is constructed without fitting parameters, using the value of $D = 0.27$ K obtained from the gap of the ESR spectrum in the $\mathbf{H} \perp \mathbf{D}$ field orientation and the $g$-factor obtained from high-temperature measurements of the ESR frequencies [18], $g = 2.24$.

However, one can see from the dependence representing the resonant fields in a wide frequency range (Fig. 6) that in stronger fields there is a significant deviation of the experimental frequency-field dependence from the predictions of the theory of noninteracting spinons, shown by dashed lines. In the region of fields and frequencies corresponding to this deviation, a significant decrease in the intensity and disappearance of the upper component of the doublet were also observed [18, 20], with the reasons being unclear.

Thus, we can summarize the introductory part by concluding that, in dielectric crystals with antiferromag-

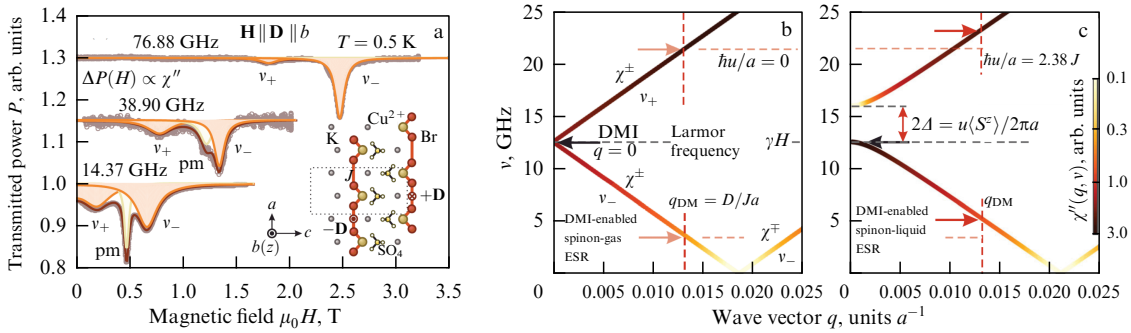


**Figure 4.** (a) Examples of dependences of microwave power transmitted through a resonator with a $K_2CuSO_4Br_2$ sample on magnetic field for three frequency values. Symbols are experimental data and solid orange lines are results of fitting of spinon doublet lines by Lorentz resonance curves. Solid gray lines are result of fitting parasitic impurity paramagnetic (pm) lines, and solid brown lines are sum of all fitting lines. Inset shows arrangement of magnetic $Cu^{2+}$ ions forming spin chains extended along $a$-axis and their surroundings; opposite directions of DMI vectors **D** in neighboring spin chains are marked. (b) Boundaries of $K_2CuSO_4Br_2$ spinon continuum in free fermion model in region of small wave vectors in the presence of a magnetic field at hypothetical value $D = 0$. In this case, ESR should be observed at Larmor frequency. Presence of $D = 0.27$ K leads to observation of ESR at frequencies $\nu_\pm$ corresponding to wave vector $q_{DM}$ in Heisenberg chain continuum. (c) Spinon continuum boundaries in spinon model with Fermi-liquid interaction and $u = 2.38Ja/\hbar$. Horizontal arrows show $\nu_\pm$ frequencies. ESR line intensities are shown in color. (©APS, figure borrowed from [7].)

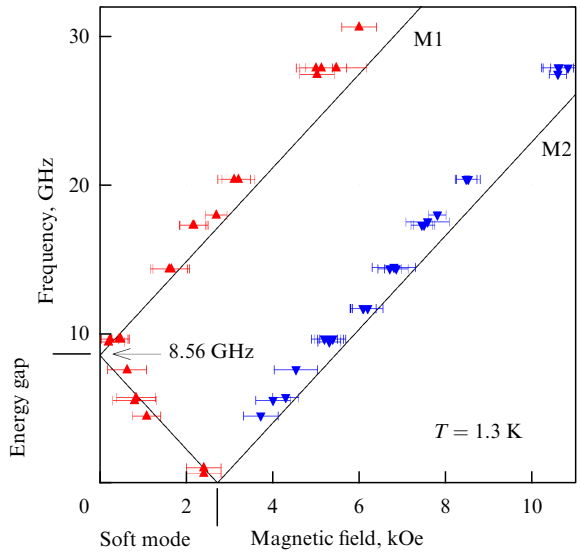


**Figure 5.** Frequency-field dependence of components of spinon doublets M1 and M2 for $K_2CuSO_4Br_2$ in low fields at $\mathbf{H} \| \mathbf{D}$. Solid lines are calculations using formula (6). (Based on materials from [18].)

netic chains of $S = 1/2$ spins, the formation of a spectrum of spin fluctuations in the form of a two-spinon continuum has been confirmed theoretically and in experiments on inelastic neutron scattering and electron spin resonance, based on transitions in the system of spin fermions filling the lower half of the Brillouin zone in the ground state. The boundaries of the continuum in the first approximation are well defined in the approximation of noninteracting fermions.

## 2. Fermi-liquid interaction of spinons

Next, we consider the issue of the interaction of spinons, the influence of which in a one-dimensional system should be expected, since collisions of delocalized quasiparticles in a one-dimensional system are inevitable. The need to analyze the interaction of spinons is stipulated by deviations from the theory of free spinons. In particular, the results of numerical experiment [21] demonstrate a discontinuity in the spectrum near the energy of the Larmor precession, increasing with the magnitude of the external field. In addition, in an experimental study of the spinon doublet in strong fields ($H \gg D/g\mu_B$) [18, 20], the coincidence with the spectrum of the spinon doublet of free fermions is violated, and an unexpected suppression of the upper component of the doublet by a strong field is observed.

The influence of the interaction of spinons on the spectrum of the continuum of excitations of the antiferromagnetic chain of spins has been recently analyzed by field-theoretical methods in [22]. Keselman et al. [22] showed that the backscattering processes lead to an additional shift of the continuum boundaries, in particular, to the appearance of a gap between the energy values at $k = 0$, and the spin oscillation mode with the Larmor energy $2g\mu_B H$ is separated by a gap

$$\Delta = \frac{\hbar u}{2a} \langle S_z \rangle \tag{8}$$

from a higher mode with an intensity that disappears at $k = 0$. The backscattering parameter $u$, which has the dimension of velocity, is introduced when writing the contribution $\hat{V}_{bs}$ to the Hamiltonian due to backscattering processes (see [7] and the Supplemental material to [7]):

$$\hat{V}_{bs} = -\frac{\hbar u}{2} \int \mathrm{d}x \, (\hat{\psi}^\dagger_{R\uparrow} \hat{\psi}_{R\downarrow} \hat{\psi}^\dagger_{L\downarrow} \hat{\psi}_{L\uparrow} + \hat{\psi}^\dagger_{R\downarrow} \hat{\psi}_{R\uparrow} \hat{\psi}^\dagger_{L\uparrow} \hat{\psi}_{L\downarrow})$$

$$- \frac{\hbar u}{4} \int \mathrm{d}x \, (\hat{\psi}^\dagger_{R\uparrow} \hat{\psi}_{R\uparrow} - \hat{\psi}^\dagger_{R\downarrow} \hat{\psi}_{R\downarrow})(\hat{\psi}^\dagger_{L\uparrow} \hat{\psi}_{L\uparrow} - \hat{\psi}^\dagger_{L\downarrow} \hat{\psi}_{L\downarrow}) \,. \tag{9}$$

Here, the operators $\hat{\psi}_{R/L,\uparrow/\downarrow}$ describe fermions with spin projections $\uparrow/\downarrow$ and wave vectors $\pm k_F$ near the right and left boundaries of the one-dimensional Fermi surface.

A nonzero value of $\Delta$ appears when the chain is magnetized ($\langle S_z \rangle$ is the average dimensionless magnetization). The effect of the spinon interaction on the continuum boundaries and the ESR frequency is illustrated in Fig. 4c.

As a result, the frequencies of the spinon doublet for the parallel orientation of the field and the Dzyaloshinskii–

Moriya vector taking into account the interaction of spinons are expressed as [7]

$$2\pi\hbar v_{\pm} = \left| g_{\parallel}\mu_{\mathrm{B}}H + \Delta \pm \sqrt{\Delta^2 + (1-\delta^2)\left(\frac{\pi D}{2}\right)^2} \right| . \quad (10)$$

Here and in this section, $\delta$ is the dimensionless interaction parameter,

$$\delta = \frac{u}{4\pi v_{\mathrm{F}}} ; \quad (11)$$

it is related to the spin susceptibility per unit length of the chain

$$\chi = \frac{1}{H}\frac{\langle S_z \rangle}{a}$$

by the relation

$$\chi = \frac{g\mu_{\mathrm{B}}a}{2\pi\hbar v_{\mathrm{F}}(1-\delta)} , \quad (12)$$

which yields the relationship between the quantities $\Delta$ and $\delta$:

$$\Delta = \frac{\delta}{(1-\delta)}\, g\mu_{\mathrm{B}}H . \quad (13)$$

Relations (10) and (13) allow one to obtain theoretical dependences of the frequencies of the spinon doublet (10) on the magnetic field and to determine the interaction parameters of the spinons $\delta$ and $u$.

Povarov et al. [7] measured in detail frequencies and intensities of the components of the spinon doublet in $K_2CuSO_4Br_2$ for $\mathbf{H} \| \mathbf{D} \| b$ at temperatures of 0.5 and 1.4 K and fitted the experimental data to the results of the described theory, which is shown in Fig. 6. Figure 6a presents the general view of the frequency-field dependence. It is evident from the figure that the deviation from the simple dependence characteristic of a gas of noninteracting fermions (dashed lines) occurs at frequencies of about 50 GHz. Figure 6b shows the experimental data and theoretical dependences for the deviation of the resonant frequency from the Larmor frequency. For a gas of noninteracting fermions, the frequency deviations from the Larmor frequency should be constant and are shown by dashed horizontal lines with ordinates of $\pm 8.3$ GHz. Theoretical fitting taking into account the Fermi-liquid interaction [relations (10) and (13)] shows excellent agreement with the experimental data for the spinon interaction parameter $\hbar u/a = 48.8$ K, which corresponds to the dimensionless parameter $\delta = 0.12$. This is the only fitting parameter, since the value $D = 0.27$ K is determined in [18] from the magnetic resonance gap in the $\mathbf{H} \perp \mathbf{D}$ orientation. In the framework of the theory [22], taking into account the interaction of spinons, the dependence of the intensity ratio of the components of the spinon doublet was also obtained, which explains the gradual disappearance of the upper component with increasing frequency:

$$\frac{I_{\nu}^{+}(H^{+})}{I_{\nu}^{-}(H^{-})} = \frac{\sqrt{(2\pi\hbar\nu\delta)^2 + \left[(1-\delta^2)(\pi D/2)\right]^2} - 2\pi\hbar\nu\delta}{\sqrt{(2\pi\hbar\nu\delta)^2 + \left[(1-\delta^2)(\pi D/2)\right]^2} + 2\pi\hbar\nu\delta} . \quad (14)$$

Here, $I_{\nu}^{+}(H^{+})/I_{\nu}^{-}(H^{-})$ is the intensity ratio at frequency $\nu$ for the components of the doublet with resonant fields $H^{+}$ and $H^{-}$, respectively.

This dependence is compared with the experimental results [7], shown in Fig. 6c. Despite the fact that no fitting parameters are used, there is good agreement. For noninteracting spinons, the ratio $I_{\nu}^{+}(H^{+})/I_{\nu}^{-}(H^{-})$ should be equal to unity and independent of the field.

Summarizing this section, we can conclude that experimental studies of the spinon doublet in $K_2CuSO_4Br_2$ demonstrate a significant interaction of spinons, which explains the spectrum of the electron spin resonance and shows that the spin-liquid state realized at a low temperature in antiferromagnetic $S = 1/2$ chains is a state of a specific Fermi liquid of collective states of spins in a dielectric crystal.

Note that the detected interaction of fermions is in a certain sense analogous to the Fermi-liquid interaction in ordinary Fermi systems such as the electron liquid in metals and normal helium-3. For electrons in a metal, the Fermi-liquid interaction leads to the appearance of Silin's spin waves [23, 24], which were observed in ESR experiments with thin samples of alkali metals [25, 26]. In liquid helium-3 at temperatures above the superfluid transition, effects of spatial correlation of spins associated with the Fermi-liquid interaction were also observed, leading to the formation of an ordered dynamic structure in the form of a uniformly precessing domain [27].

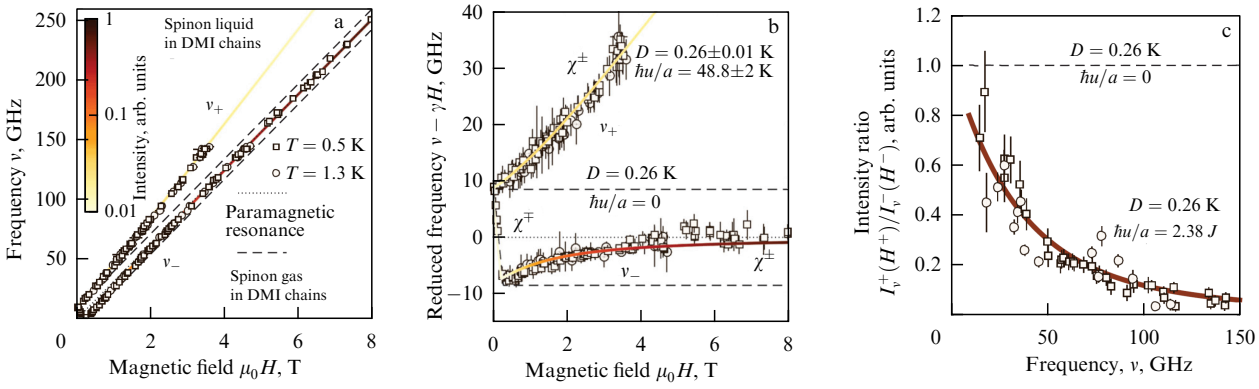


**Figure 6.** (a) Frequency-field dependence of components of spinon doublet. (b) Deviation of frequencies of components of spinon doublet from Larmor frequency. Symbols are experimental data, solid lines are theory, and ESR signal intensity is shown by changing line color according to intensity scale. (c) Frequency dependence of intensity ratio of upper and lower components of $I^{+}/I^{-}$ doublet. Symbols are experimental results, and solid line is drawn according to theory, formula (14). (©APS, figure borrowed from [7].)

## 3. Study of excitation spectrum of $S = 1/2$ XXZ chains in quasi-one-dimensional antiferromagnet $Cs_2CoCl_4$

Heisenberg $S = 1/2$ antiferromagnetic chains are surely most strongly affected by quantum fluctuations. Other systems, in which anisotropy or a magnetic field suppress fluctuations, exhibit spin structures that are intermediate between antiferromagnetically ordered structures and quantum-disordered spin-liquid states. Consider an antiferromagnetic $S = 1/2$ chain with anisotropy, in which the effective exchange interaction has an anisotropic additive that distinguishes it from the canonical Heisenberg exchange. Let the resulting symmetry of the system without a magnetic field be uniaxial. This model system is called an XXZ chain, the $z$-axis in spin space being easy-axis anisotropy. In the case of easy-plane anisotropy and in a transverse (so-called noncommuting) field $H = H_x$, theoretical analysis [28–31] reveals a variety of exotic ground states. In a zero field, it is a quantum-critical spin liquid; in a magnetic field $H = H_x$, it is a flopped antiferromagnet with long-range magnetic ordering; in a critical magnetic field, the antiferromagnetic order is vanished and the state of the spin liquid for the transverse components of the spins is restored; and, finally, with a further increase in the field, magnetic saturation is achieved only asymptotically in this 'noncommuting' orientation of the magnetic field, violating the axial symmetry of the problem. In the ordered phase, the ordered components of the spin are strongly reduced by quantum fluctuations. It seems at first glance that the conditions of exchange anisotropy and $S = 1/2$ are incompatible, since the spin-1/2 is not subject to the action of single-ion anisotropy. However, in crystals with magnetic ions of the $S = 3/2$ spin and strong single-ion easy-plane anisotropy, the upper $S_z = \pm 3/2$ spin sublevels lie high and are not populated at low temperatures. All magnetic properties are determined by the lower doublet $S_z = \pm 1/2$, and the system can be described in the representation of $s = 1/2$ pseudospins. In this case, the anisotropic properties of the system are effectively preserved and effective anisotropy of the exchange interaction arises in the spin Hamiltonian. In particular, for $Cs_2CoCl_4$ crystals, the magnetic $Co^{2+}$ ions have an $S = 3/2$ spin, and the single-ion anisotropy parameter is $D = 7$ K, while the exchange integral between the spins in the chains is $J_{3/2} = 0.74$ K [31]. The easy anisotropy plane for different Co ions is directed differently (see the sketch of the crystal structure in [32]), but the easy anisotropy plane contains the crystallographic $b$-axis for all ions, and this can be chosen as the 'noncommuting' direction of the magnetic field $H_x$. The spin chains with the largest exchange integral are extended along the $b$-axis. The initial $S = 3/2$ spin Hamiltonian of the chain has the form

$$\mathcal{H} = \sum_i \left( J_{3/2} \mathbf{S}^i \mathbf{S}^{i+1} + D(S_z^i)^2 + g_{3/2} \mu_B \mathbf{H} \mathbf{S}^i \right). \qquad (15)$$

At low temperatures, we can make use of the representation of pseudospins $s$, and Hamiltonian (15) takes the form [33]

$$\mathcal{H} = \sum_i \left( J_{1/2} (s_x^i s_x^{i+1} + s_y^i s_y^{i+1}) + \Delta s_z^i s_z^{i+1}) + g_{1/2,\alpha} \mu_B H_\alpha s_\alpha^i \right), \qquad (16)$$

where $s_\alpha^i$ are the operators of the components of $s = 1/2$ pseudospins on the lattice sites $i$, $g_{1/2,\alpha}$ are the components of the $g$ tensor, and $H_\alpha$ are the components of the magnetic field vector. The exchange integral undergoes renormalization $J_{1/2} = 4J_{3/2}$. In the limiting case $D \gg J_{3/2}$, the remaining parameters are $\Delta = 0.25$, $g_{1/2,x} = 2g_{3/2}$. For $Cs_2CoCl_4$ crystals, $J_{3/2} = 0.74$ K, $D = 7$ K, and the calculated values of the above parameters are equal to [30, 31]

$$\Delta \simeq 0.25 \left( 1 - \frac{39 J_{3/2}}{D} \right) = 0.12 ,$$
$$g_{1/2,b} \simeq 2 g_{3/2} \left( 1 - \frac{3}{2} \frac{J_{3/2}}{D} \right) = 3.3 . \qquad (17)$$

The XXZ chains in theoretical studies [28, 33] exhibit a remarkable spectrum of $S = 1$ excitations. In the zero field, it has the form of a continuum, practically identical to the spectrum of the Heisenberg $S = 1/2$ antiferromagnetic chain. In a magnetic field near $k = 0$, a gap appears inside the continuum, very similar to that described in Section 2 (see Fig. 4). In this case, the continuum continues to exist in the region of fields where the long-range magnetic order exists. This type of spectrum allows one to assume that excitations in the chains in question have a character close to the spinonic one. In the critical field $H_c = 1.6 J_{1/2}/(g_{1/2}\mu_B)$, resonant branches of excitations arise, and an energy gap opens on the wave vector $k = \pi/a$, increasing with magnetic field. Data on the described spectrum were obtained by numerical simulations using the density matrix renormalization group (DMRG) method and are presented as a color image of the structure factor on the wave vector–energy plane for different polarizations of the transferred moment and a dense series of magnetic field values (see Supplemental Material to paper [28]). A comparison of the continua obtained by Laurell et al. [28] and Bruognolo et al. [33] for $\Delta = 0.25$ and 0.12, respectively, shows that a change in the parameter $\Delta$ within the specified limits does not significantly affect the spectrum parameters. When studying the ESR spectra in $Cs_2CoCl_4$ crystals, we set ourselves the task of checking experimentally the formation of a system of pseudospins with a characteristic value of the $g$-factor at temperatures below $D/k_B$. With a further decrease in temperature, the aim is to track changes in the spectrum during the formation of a correlated state of spin chains, and with even deeper cooling (below 0.2 K), we track the formation of spectra of a three-dimensional ordered phase. We will describe the results of the performed experiments, following paper [34].

The ESR spectra in the temperature range from 7 to 0.1 K were investigated using an original microwave spectrometer integrated with a dilution microcryostat with an autonomous sorption pump [35]. Figure 7 shows the temperature evolution of the ESR signal at a frequency of 40.99 GHz for $\mathbf{H} \parallel b$, i.e., in a noncommutating, transverse orientation of the magnetic field. In the temperature range $2 < T < 3$ K, a single resonance line is observed in the field $H_1 = 8.9$ kOe, corresponding to a $g$-factor of 3.3, in agreement with formula (17) for a pseudospin state with a renormalized $g$-factor value. Upon further cooling at a temperature below 2 K, a second ESR line appears near the field $H_2 = 12.5$ kOe, the intensity of which increases upon cooling and predominates at $T < 1$ K. Below the three-dimensional ordering temperature (0.3 K) in a field of 12 kOe [32], the ESR line narrows sharply, and additional satellites appear (A, B, C, and D in Fig. 7). This temperature evolution shows, first, the formation of a pseudospin state with a specific value of the $g$-factor, then reveals a smooth change in the spin state of the crystal at a

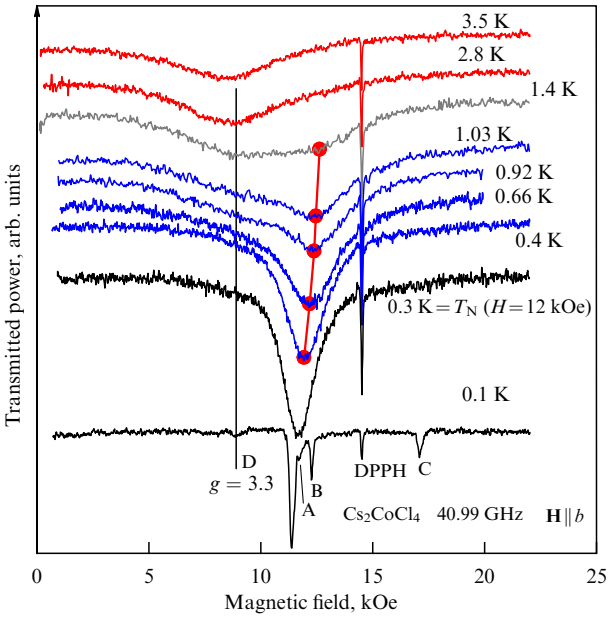


**Figure 7.** Examples of ESR lines measured in $Cs_2CoCl_4$ at frequency of 40.99 GHz for $\mathbf{H} \| b$. (Based on materials from [34].)

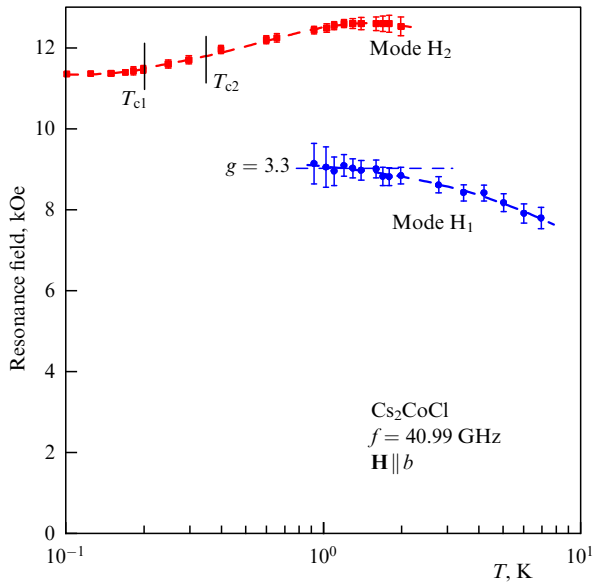


**Figure 8.** Dependences of resonance fields $H_1$ and $H_2$ at frequency of 40.99 GHz on temperature for $\mathbf{H} \| b$ in $Cs_2CoCl_4$ samples. $H_1$ is ESR field of uncorrelated pseudospins, and $H_2$ is ESR field of spin-liquid state. $T_{c1}$ and $T_{c12}$ are critical temperatures for occurrence of ordered phases according to [32]. (Based on materials from [34].)

temperature on the order of $J_{1/2}/k_B$, and, finally, shows a change in the spectrum of spin excitations at a three-dimensional ordering temperature of 0.3 K. The change in the ESR fields with temperature is shown in Fig. 8, where the transition from the resonance of uncorrelated pseudospins with $g = 3.3$ to that of the correlated state of the chain is clearly visible. To diagnose the state arising in the temperature range $0.3 < T < 1$ K, we traced the frequency-field dependence of the ESR, for which absorption lines were recorded at a number of frequencies in the range of 25–120 GHz. Comparing the frequency-field dependences for the ESR of disordered pseudospins (at a temperature of 3–4 K)

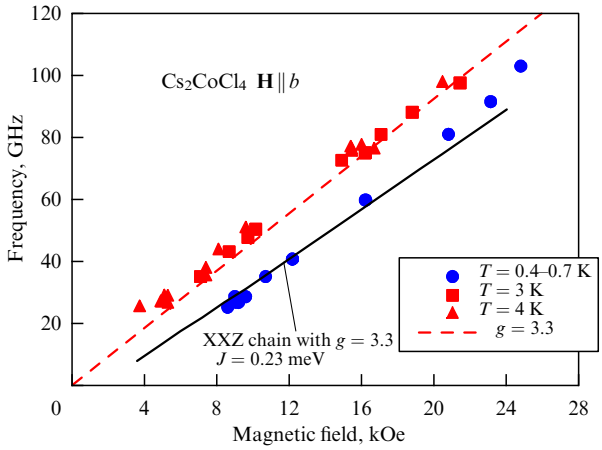


**Figure 9.** Frequency-field dependence of spin resonances for $\mathbf{H} \| b$ in spin-liquid phase of $Cs_2CoCl_4$. Dashed line shows theoretical dependence corresponding to $g$-factor of 3.3. Solid line is theoretical dependence according to calculations [28]. (Based on materials from [34].)

and in the correlated phase (at a temperature of 0.3–0.4 K) is shown in Fig. 9. For temperatures of 3–4 K, the frequency-field dependence corresponds to a $g$-factor of 3.3 (dashed line). To identify the ESR frequencies in the temperature range of 0.3–0.4 K, we compare the experimental data with the theoretical values (borrowed from [28] and Supplemental material to that paper) of the lower mode frequency of the XXZ chain spin oscillations at a zero wave vector. To this end, we recalculate the magnetic field given in [28] in units of the exchange integral into a real field using the above value of $J_{1/2}$ and the experimentally determined value of $g = 3.3$. The resulting theoretical dependence, in which there are no adjustable parameters, is shown in Fig. 9 by a solid curve. The frequency of the upper mode of spin oscillations, which also has a maximum of the structure factor in [28], is not shown here, since this mode has almost a zero intensity at a zero wave vector. One can see that, in the entire frequency range, there is good agreement between the observed ESR frequencies and the calculated values of the lower boundary of the continuum for the XXZ antiferromagnetic chain of $S = 1/2$ spins.

Thus, we can conclude that the spin structure of the ground state of the XXZ chain with a spectrum corresponding to the spinon continuum calculated numerically in [28] is realized in the chains in $Cs_2CoCl_4$ crystals in the intermediate temperature range between the temperature of three-dimensional ordering and that of the occurrence of intrachain correlations $T \simeq J_{1/2}/k_B$. In this case, interchain correlations and three-dimensional order are still absent, since the energy of the interchain exchange of pseudospins is very small and is estimated to be 0.035 K [36]. Upon decreasing the temperature below 0.3 K and evolving to a three-dimensional ordered state, the ESR spectrum undergoes another rearrangement, which will be described elsewhere, together with the antiferromagnetic resonance of the ordered phase.

## 4. Conclusions

We have studied experimentally magnetic resonance in quasi-one-dimensional Heisenberg and anisotropic $S = 1/2$ antiferromagnets and have found the effect of the Fermi-liquid interaction of spinons in the Heisenberg antiferromagnetic

chain on the spinon spectrum. This effect manifests itself in an additional shift of the spinon continuum boundaries in a magnetic field. For an anisotropic chain antiferromagnet, a crossover of the ESR spectrum of uncorrelated pseudospins to the ESR of spinons in the XXZ chain has been observed.

This paper builds on the results of the work reported in Refs [7, 34]. I sincerely thank all the coauthors of these papers for our long-term close cooperation: A. Zheludev, K.Yu. Povarov, T.A. Soldatov, O.A. Starykh, and V.S. Edelman.

The work was supported by the Russian Science Foundation (grant number 22-12-00259) and the State Order of the P.L. Kapitza Institute of Physical Problems of the Russian Academy of Sciences.

## References

1. Bethe H *Z. Phys.* **71** 205 (1931)
2. Faddeev L D,Takhtajan L A *Phys. Lett. A* **85** 375 (1981)
3. Dender D C et al. *Phys. Rev. Lett.* **79** 1750 (1997)
4. Bonner J C, Fisher M E *Phys. Rev.* **135** A640 (1964)
5. Fadeev L D *Phys. Usp.* **56** 465 (2013); *Usp. Fiz. Nauk* **183** 487 (2013)
6. Smirnov A I *Phys. Usp.* **59** 564 (2016); *Usp. Fiz. Nauk* **186** 633 (2016)
7. Povarov K Yu, Soldatov T A, Wang R-B, Zheludev A, Smirnov A I, Starykh O A *Phys. Rev. Lett.* **128** 187202 (2022)
8. Dender D C "Spin dynamics in the quasi-one-dimensional $S = 1/2$ Heisenberg antiferromagnet copper benzoate," PhD Thesis (Baltimore, MD: The Johns Hopkins Univ., 1998); Dissertation Abstracts Intern., Vol. 59-01, Sect. B, Publ. Number: AAI9821113
9. des Cloizeaux J, Pearson J J *Phys. Rev.* **128** 2131 (1962)
10. Coldea R, Tennant D A, Tylczynski Z *Phys. Rev. B* **68** 134424 (2003)
11. Tennant D A et al. *Phys. Rev. B* **52** 13368 (1995)
12. Lake B et al. *Phys. Rev. Lett.* **111** 137205 (2013)
13. Dzyaloshinsky I *J. Phys. Chem. Solids* **4** 241 (1958)
14. Moriya T *Phys. Rev.* **120** 91 (1960)
15. Gangadharaiah S, Sun J, Starykh O A *Phys. Rev. B* **78** 054436 (2008)
16. Karimi H, Affleck I *Phys. Rev. B* **84** 174420 (2011)
17. Povarov K Yu, Smirnov A I, Starykh O A, Petrov S V, Shapiro A Ya *Phys. Rev. Lett.* **107** 037204 (2011)
18. Smirnov A I et al. *Phys. Rev. B* **92** 134417 (2015)
19. Hälg M et al. *Phys. Rev. B* **90** 174413 (2014)
20. Smirnov A I et al. *Phys. Rev. B* **91** 174412 (2015)
21. Kohno M *Phys. Rev. Lett.* **102** 037203 (2009)
22. Keselman A, Balents L, Starykh O A *Phys. Rev. Lett.* **125** 187201 (2020)
23. Silin V P *Sov. Phys. JETP* **6** 945 (1958); *Zh. Eksp. Teor. Fiz.* **33** 1227 (1957)
24. Silin V P *Sov. Phys. JETP* **8** 870 (1959); *Zh. Eksp. Teor. Fiz.* **35** 1243 (1958)
25. Platzman P M, Wolff P A *Phys. Rev. Lett.* **18** 280 (1967)
26. Schultz S, Dunifer G *Phys. Rev. Lett.* **18** 283 (1967)
27. Dmitriev V V, Fomin I A *JETP Lett.* **59** 378 (1994); *Pis'ma Zh. Eksp. Teor. Fiz.* **59** 352 (1994)
28. Laurell P et al. *Phys. Rev. Lett.* **127** 037201 (2021)
29. Kurmann J, Thomas H, Müller G *Physica A* **112** 235 (1982)
30. Kenzelmann M et al. *Phys. Rev. B* **65** 144432 (2002)
31. Breunig O et al. *Phys. Rev. Lett.* **111** 187202 (2013)
32. Breunig O et al. *Phys. Rev. B* **91** 024423 (2015)
33. Bruognolo B et al. *Phys. Rev. B* **94** 085136 (2016)
34. Soldatov T A, Edelman V S, Smirnov A I *Appl. Magn. Res.* **55** 1137 (2024)
35. Smirnov A I, Soldatov T A, Edelman V S *Instrum. Exp. Tech.* **65** 668 (2022); *Prib. Tekh. Eksp.* (4) 131 (2022)
36. Yoshizawa H et al. *Phys. Rev. B* **28** 3904 (1983)